Proceedings World Geothermal Congress 2023
Beijing, China, April 17 – 21, 2023

Potential of Natural Recharge Lahendong Geothermal Field Calculated by Surface Water Availability Concept and Fault Fracture Density

Ristio Efendi, Antonius Rishang Untoro, Sigit Suryanto, Teza Permana

PT. PERTAMINA GEOTHERMAL ENERGY

Grha Pertamina Building 5th Floor, Medan Merdeka Timur St. No. 11-13 Jakarta 10110

Ristio.efendi@pertamina.com

Keywords: Natural Recharge, Isotope, Lahendong

ABSTRACT

The geothermal system relies heavily on natural recharging. Natural recharge has both positive and negative impacts in geothermal systems. There are many unanswered issues about natural recharge studies in geothermal fields, particularly in the Lahendong field, which include the age of recharge water, the amount of recharge volume, the movement path, and more.

This study attemted to calculate the amount of natural recharge volume by using the natural isotope approach of ^{18}O and ^{2}H to obtain the reservoir fluid correlation with elevation on the surface, then combining fault fracture density analysis to observe zones of possible water recharge infiltration in the ground. Later in this study, the amount of infiltration water derived from rain is determined at a one-year interval.

Two approaches were assessed in order to calculate the amount of water that percolates through the earth. Approximately 1 megaton of recharge water entered the Lahendong geothermal reservoir, which was proven by positive anomalous micro gravity monitoring

1. INTRODUCTION

The Lahendong geothermal field is located 40 kilometers south of Manado in the district of Tomohon, Minahasa, North Sulawesi (Figure 1). The field is typically located between 600 and 900 meters above sea level. Lahendong geothermal is one of Indonesia's major geothermal resources. It is located within the Lahendong WKP, which also includes a tompaso field. The area is characterized by active vulcanoes that create Minahasa's volcanic inner arc, which is tectonically active.

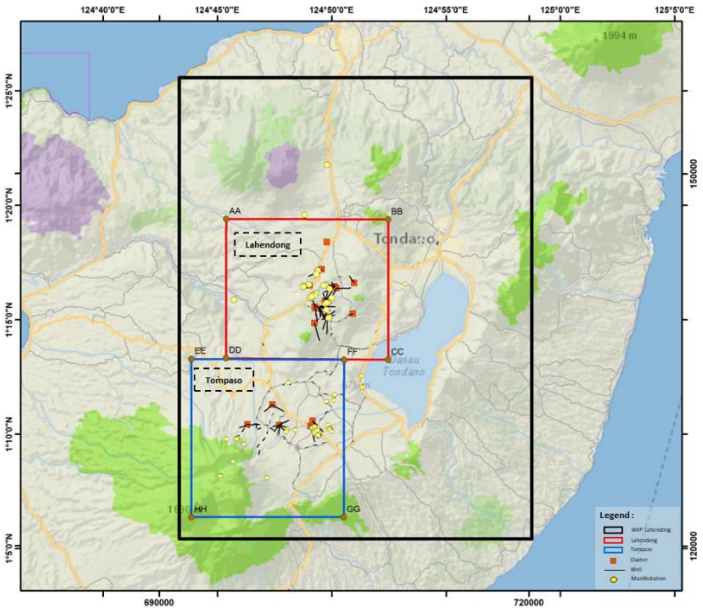

Figure 1: Location map of Lahendong and Tompaso geothermal field

Pertamina has drilled 39 wells that will generate 6x20 Mwe until 2022. Unit I, which generates 20 MWe, was commissioned in 2001 and has been continuously working since then. The development of 40 MWe was commissioned between 2007 and 2009, with the final 20 MWe commissioned in 2011. Lahendong's current capacity generation is 80 MWe from four power plants and 2x20 MWe generated at Tompaso, which is also included in the Lahendong WKP. The Lahendong Field is a two-phase geothermal reservoir with two distinct reservoir zones. The southern reservoir has temperatures ranging from 300° to 350° C and a dryness of approximately 80%, whereas the northern reservoir has lower temperatures ranging from 250° to 280° C and a dryness of approximately 30%. (Koestono, 2010).

In order to maintain a mass balance within the reservoir, it is necessary to conduct a recharge study in Lahendong geothermal field. The main objective of this study is to predict the amount of natural recharge within the given area by means of an overlay of the geological map, fracture density map of the investigated area.

2. GEOLOGICAL REVIEW OF LAHENDONG

The Lahendong geothermal area is distinguished by active volcanoes that compose Minahasa's volcanic inner arc, including Mt. Soputan, Mt. Lokon-Empung, Mt. Mahawu and Mt. Klabat, and Mt. Dua Saudara, all of which trend southwest to northeast. The area is structurally composed of significant strike-slip faults trending NE-SW, NW-SE, and normal faults trending N-S.

The most faulted area is west of Pangalombian caldera (around Lake Linow). The active strike slip left lateral fault, trending NE-SW, is located on the top of a volcanic inner arc of Minahasa, aligning from Mt. Soputan on the south-west side to Mt. Klabat on the northeast side. This fault directs the development of the Tondano and Pangalombian calderas and divides the geothermal system of the Lahendong field and Tompaso field. The eastern rim of the Tondano caldera may be identified where the western and southern rims were covered by lava from Mt. Lengkoan, Mt. Sempu, and Soputan (Siahaan et al., 2005).

The Lahendong geothermal field's volcano-stratigraphy is categorized into three primary rock units: the Pre-Tondano unit, the Syn-Tondano unit, and the Post Tondano unit. Furthermore, the Pre-Caldera and Post-Caldera activity of the Pangolombian caldera divide the Post-Tondano unit into two volcanic products. The Pangolombian formation and Lengkoan formation represent pre-caldera volcanic products, while the Kasuratan formation, Tampusu formation, Kasuan formation, Linow formation, and Masarang formation comprise post-caldera volcanic products. The Lahendong geothermal field and its surroundings are covered in volcanic rocks.

2. METHOD

There are at least four primary components in a geothermal system: heat source, geothermal reservoir, discharge area (manifestation), and infiltration area (recharge). It is critical to identify catchment regions in order to ensure the long-term viability of geothermal water use. Natural isotopes of circulating water in the examined area were one of the approaches used. Water isotopes of hydrogen and oxygen are used as tracers to study hydrogeological processes such as precipitation, groundwater infiltration, groundwater and surface water interactions, and basin hydrology (Gat, 1996; Clark and Fritz, 1997; Vandenschrick et al., 2002; Deshpande et al., 2003; Gibson et al., 2005; Gammons et al., 2006; Palmer et al., 2007; Blasch and Bryson, 2007; Kumar et al., 2008; Li et al., 2008).

The ratio of oxygen and hydrogen isotopes in groundwater remains constant at steady temperature as long as there is no phase shift throughout the flow. It also indicates that the isotopic state is a permanent natural tracer that records the original status of meteoric water precipitation (Senturk et al. 1970; Perry et al. 1980, Clark and Fritz 1997). We can identify the groundwater recharge area as well as the water sources that contribute to a certain area after gathering information on meteoric water and the stable isotopes of oxygen and hydrogen in groundwater, as well as assessing the hydrogeological structure and groundwater flow in the target area. Furthermore, researching isotope studies will aid in identifying groundwater recharge zones (Duplessy et al., 1980; Payne and Yurtsever, 1974; Hennig et al., 1983).

Changes in oxygen and hydrogen isotopes occur in the hydrological environment due to kinetic fractionation in seawater evaporation and rainfall condensation. Water isotopes have distinct vapor pressures and diffusion rates in these two processes, causing isotope fractionation. The proportion of oxygen and hydrogen isotopes in rainwater varies depending on the ocean in which it is generated. Diverse degrees of isotope fractionation cause different variations that can be utilized as natural markers to help us understand changes in oxygen and hydrogen isotopes from evaporation to condensation, rainfall formation, and eventually aquifer infiltration. The lighter isotopes evaporate during evaporation, enriching the remaining water with the heavier isotopes. The relative humidity and air temperature in the area where evaporation occurs also influence evaporation-induced enrichment (Van Der Straaten and Mook, 1983). However, fluctuations in isotopic composition occur during condensation as a result of temperature, terrain, altitude, and distance traveled.

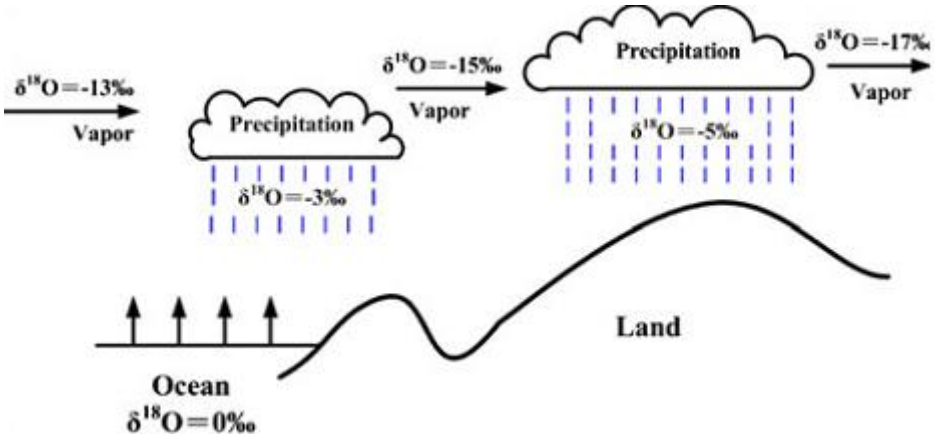

Figure 2 : Schematic of distillation effect for meteoric water (After Sharp 2007)

A series of isotopic fractionation generates isotopic changes in continental meteoric water during the evaporation of seawater into precipitation. Because the isotope equilibrium mechanism in evaporation and condensation produces a specific isotope distribution in rainfall that falls in different regions, fractionation occurs. Craig (1961) established this distribution rule while analyzing the

isotopic composition of oxygen and hydrogen in precipitation (rainwater), snow, and river water samples from throughout the world using the linear regression approach. This discovery is known as the Global Meteoric Water Line (GMWL):

$$\delta D = 8\delta^{18}O + 10$$

The same results were found in a follow-up study by the IAEA (International Atomic Energy Agency), which collected water samples from all of its rainfall stations around the world (Gal, 1980):

$$\delta D = (8.17 \pm 0.08)\delta^{18}O + (10.65 \pm 0.64)$$

Almost all precipitation on the planet follows it. However, various evaporation and condensation conditions (related to temperature and humidity) or unique habitats result in distinct meteoric waterline features with different slopes and intercepts (Senturk et al., 1970; Sakai and Matsubaya, 1977; Gat, 1980; Darling and Armansson, 1989). On North America, D = 7.95 18O + 6.03 (Gat, 1980); in tropical islands, D = 6.17 18O + 3.97 (Gat, 1980); and in Japan, D = 8 18O + 17.5 (Gat, 1980). (Sakai and Matsubaya, 1977).

Isotopes of water as a natural tracer

Six ombrometers have been placed around the Lahendong field, ranging in elevation from 197 to 1023 masl. One ombrometer is used for daily regular rainfall monitoring, while the other is checked every 2 weeks to 1 month to a whole year to reflect the rainy and dry seasons in the Lahendong area. Every month, rainwater isotope samples were collected from each ombrometer for precipitation reference, and isotope samples were also collected at two shallow wells for infiltration reference and three river locations for run off reference. All samples were analyzed at the laboratory, and quality control was accomplished. The ground water recharge proportion will be estimated using the data of deuterium and oxygen 18 analyses from run off, ground water, and rainfall. Another type of rainfall data is acquired by BMKG and used for quality control rainfall data. The local meteoric water line (LMWL) is divided into two parts, rainy season and dry season, and then averaged to provide a representative LMWL.

Hydrogen and oxygen isotopes of water are used as tracers to understand hydrogeological processes such as precipitation, groundwater infiltration, groundwater and surface water interactions, as well as basin hydrology (Gat, 1996; Clark and Fritz, 1997; Vandenschrick et al., 2002; Deshpande et al., 2003; Gibson et al., 2005; Gammons et al., 2006; Palmer et al., 2007; Blasch and Bryson, 2007; Kumar et al., 2008; Li et al., 2008).

The isotopic composition of groundwater is the same as the mean isotope weight of infiltration sources such as the composition of annual precipitation and river water. Deviation of the isotope ratio of groundwater to precipitation due to mixing with river water. This mixing also provides basic information about the absorption mechanism (Clark and Fritz, 1997).

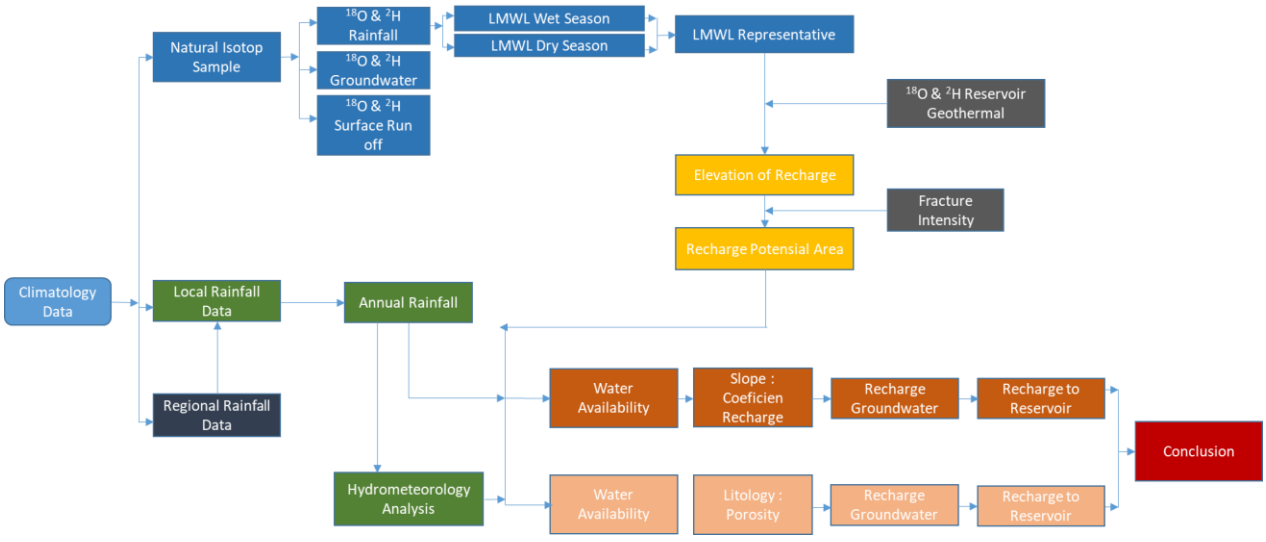

Figure 3: Flow chart diagram to calculate potensial recharge to reservoir

3. RESULT AND DISCUSSION

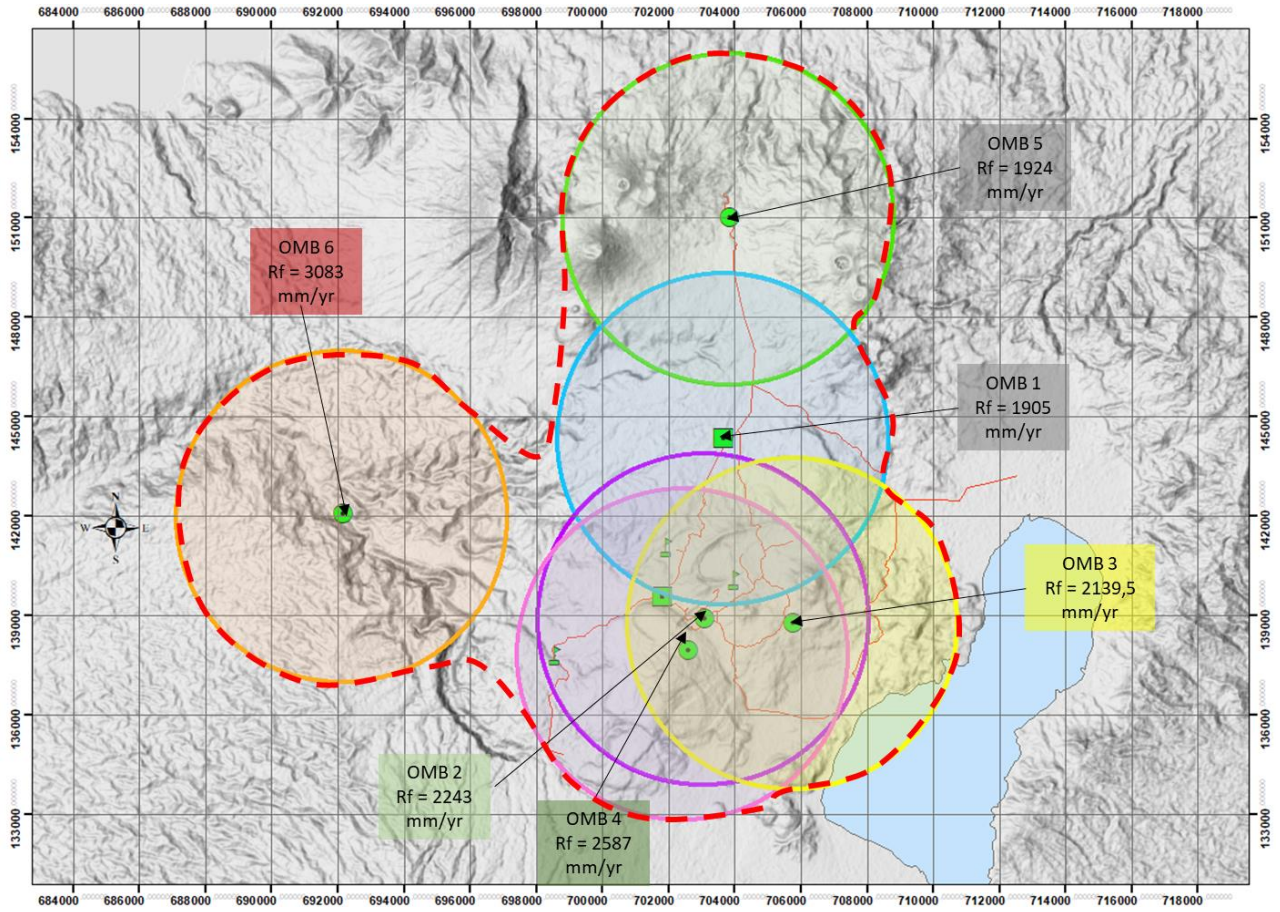

Figure 4: The observed area which assumed has same effect of rainfall (radius 5 km)

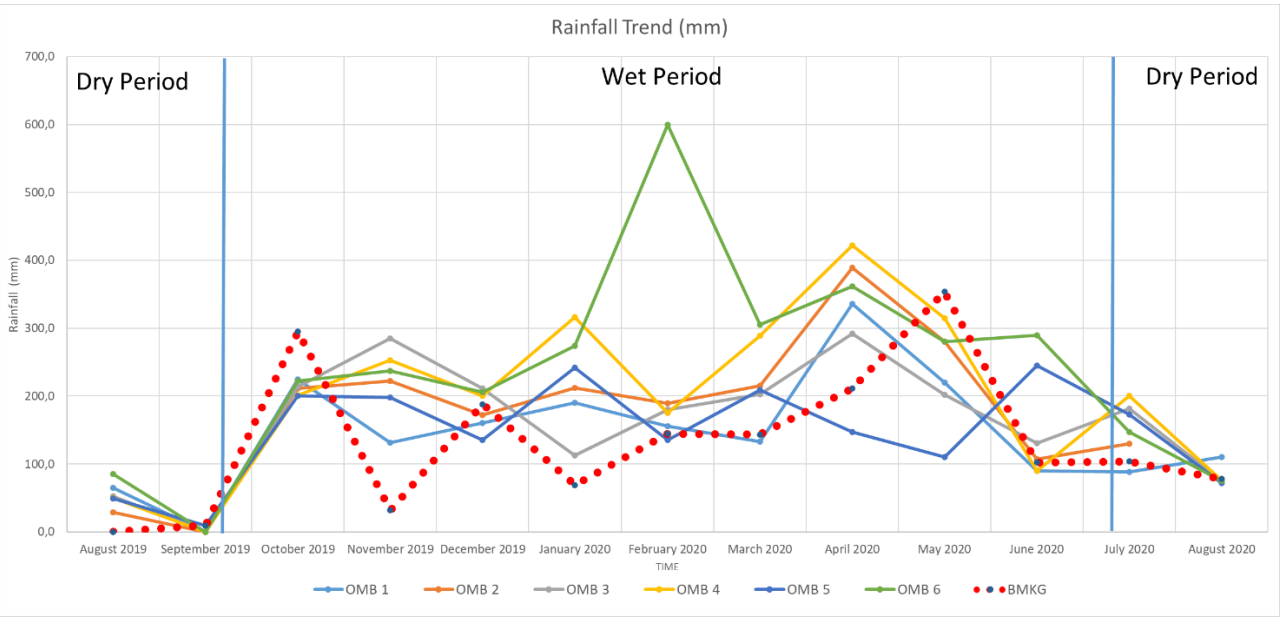

Figure 5: Rainfall trend of each ombrometer in one year period

Rainfall for each ombrometer observed from August 2019 to August 2020 has various values but exhibits the same trend, notably from July to September, which is a dry month with rainfall less than 100 mm/month, and from October to June, which is a wet month with rainfall greater than 100 mm per month. Rainfall from the BMKG station follows a similar pattern but has different values. A more precise computation involves an ombrometer and uses local rainfall observed in each ombrometer assuming the same effect, hence a radius of 5 km, so that rainfall in a 25 km^2 area is addressed the same. The median value of the two data points is used for locations that are close together or overlap with other ombrometers. The area to be determined for the water potential is the red dotted line region (Figure

3.1 Elevation of Recharge

A catchment area study in Lahendong was previously conducted in 2014. Additional research is being conducted to determine the recharge zone and recharge potential value. The most recent data for 2019-2020 cover both the dry and wet seasons. With more extensive data, this has an impact on the local meteoric waterline equation at Lahendong. The equation is as follows based on the 18O vs D plot:

$$\delta D = 8.03\ \delta^{18}O(‰) + 12.80$$

There is a slight variance in intercept with the global meteoric waterline equation. This intercept shifting could be a consequence of new data, particularly from Lahendong, being utilized to adjust the global equation. Fundamentally, this equation is a global reference equation, however there is a local shift based on geographical location.

In this study, we also include data for river water, which is representative of surface water. We also included data from a well's shallow ground water, which indicates isotop infiltration. Both data are located on the local meteoric water line, which reveals that no fractionation occurs as long as rainwater penetrates the soil and becomes groundwater. Thus, we obtain the isotope value of the water supplying Lahendong's underground water. This isotope value serves as a reference for the shift in water temperature experienced by both manifestations and geothermal wells.

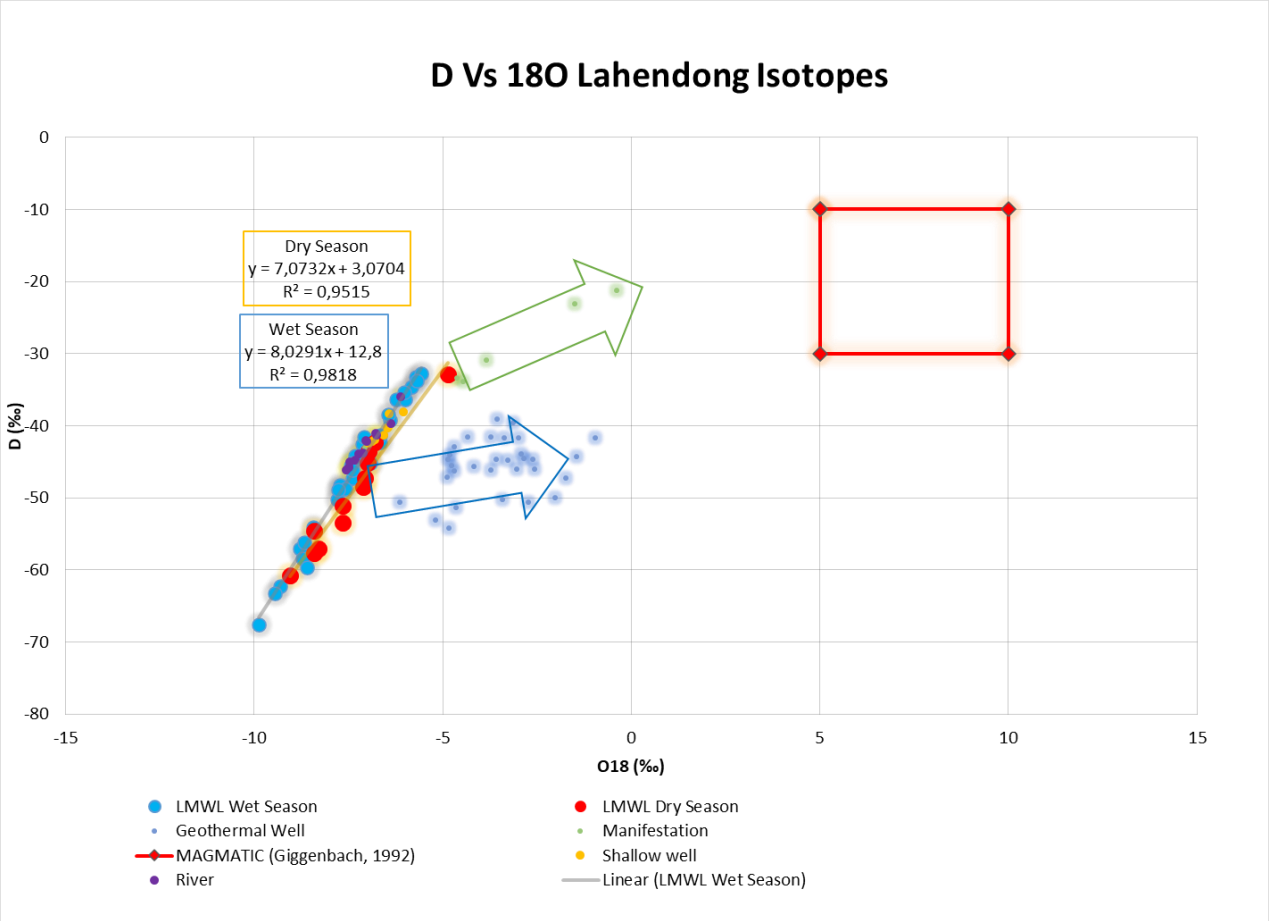

Figure 6: Local Meteoric Water Line (LMWL) Lahendong and shifting isotopes value of geothermal fluid

The isotope of manifestation water is taken from the surface thermal manifestation which dominated by steam heated water. Meanwhile, isotopes of water from geothermal wells are derived from periodic monitoring data collected since the field's establishment. Geothermal reservoir fluid is a fractionated fluid caused by the pressure drop as the water rises through the well. As a consequence, corrections are applied to the geothermal fluid in order to obtain the value in the reservoir.

We utilize the Deuteurium vs. Elevation plot using rainwater data to calculate the elevation of the catchment region. Then we take the deteurium value from the geothermal well water, which is in the range of -39 to -54. The elevation of the catchment region is derived at approximately 750-900 masl by applying this range of values to the deuterium vs. elevation line equation.

3.2 Recharge potential area

The elevation of recharge derived from isotope data is converted into an elevation map that is filtered to an elevation of 750-900 masl, then combined with a fracture density map for the Lahendong area, and the overlay zone between high density fracture (yellow-red) and elevation recharge generates the recharge potential area (blue zone). There are 16 recharge potential areas recognized, with locations and areas as displayed in the image below:

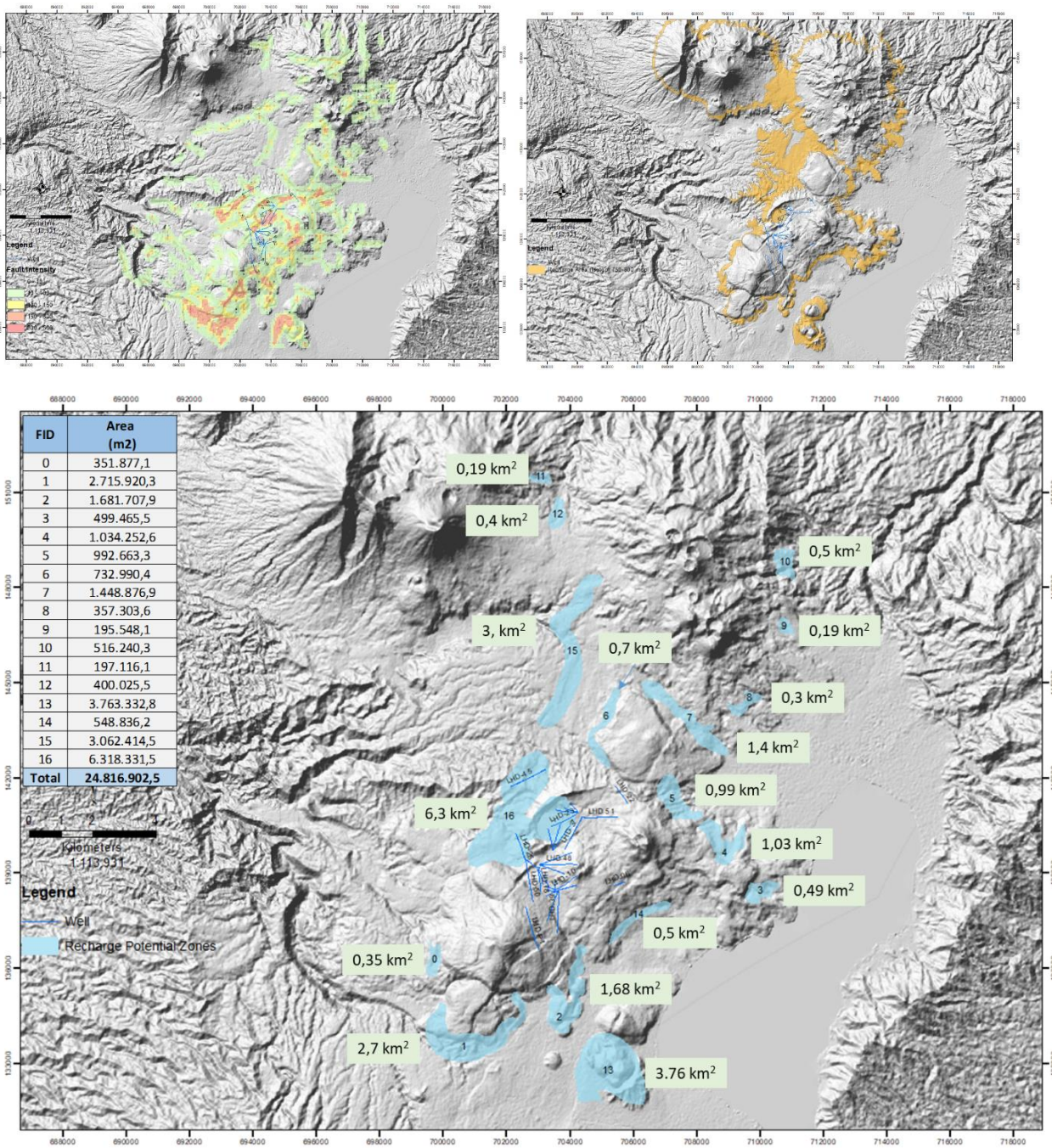

Figure 7: Recharge Potential Area in Lahendong field

3.3 Amount of Recharge Potential

The rainfall data utilized in the calculation is the rainfall of each ombrometer, which assumes a certain amount of water falls to a recharge potential area. The calculation exercise with porosity lithology 41% (based on data xxx) and reservoir Lahendong porosity 8% is based on utilizing two alternative ways to compute the infiltration value and the amount of water recharged in the Lahendong field.

3.3.1 Method 1 (Hydrometeorology analysis)

Component	August	September	October	November	December	January	February	March	April	May	June	July
Rainfall (RF)	65	0	225	132	161	190	156	133	336	220	90	88
Category	DM	DM	WM	WM	WM	WM	WM	WM	WM	WM	DM	DM
Number of Rainy Days	5	0	12	17	19	20	21	17	28	27	15	13
Number of Dry Days	25	31	19	13	12	11	8	14	2	4	15	18
Potential Evapotranspiration (PET)	26,62	26,62	26,62	26,62	26,62	26,62	26,62	26,62	26,62	26,62	26,62	26,62
Limited Evapotranpiration (LE)												
m	0,1	0,1	0,15	0,15	0,15	0,15	0,15	0,15	0,15	0,15	0,15	0,15
ΔE (mm/month)	1,73	2,40	1,20	0,20	-0,20	-0,40	-0,60	0,20	-2,00	-1,80	0,60	1,00
LE = PET - ΔE (mm/month)	24,89	24,23	25,43	26,42	26,82	27,02	27,22	26,42	28,62	28,42	26,03	25,63
Water Surplus												
water surplus (WS) = RF - LE	40,11	-24,23	199,57	105,08	133,68	162,98	128,78	106,58	307,38	191,58	63,97	62,37
Infiltration												
Porosity (K)	0,41	0,41	0,41	0,41	0,41	0,41	0,41	0,41	0,41	0,41	0,41	0,41
Infiltration (in 1 m square)	16,44	-9,93	81,83	43,08	54,81	66,82	52,80	43,70	126,03	78,55	26,23	25,57
Perhitungan Volume Simpan												
Coefficient (Cn)	338,34	354,16	299,11	322,36	315,32	308,11	316,53	321,99	272,59	301,08	332,47	348,20
Storage Volume (Vn)	845,85	885,41	747,77	805,89	788,30	770,28	791,31	804,97	681,47	752,69	831,17	870,51
Storage Volume previous month (Vn - 1)	832,00	845,85	885,41	747,77	805,89	788,30	770,28	791,31	804,97	681,47	752,69	831,17
2*K (Groundwater flow coefficient)	1,20	1,20	1,20	1,20	1,20	1,20	1,20	1,20	1,20	1,20	1,20	2,20
Run Off Calculation												
Base Flow	2,60	-49,50	219,46	-15,04	72,40	84,84	31,77	30,04	249,52	7,33	-52,25	-13,77
Direct Run Off	23,66	-14,29	117,75	61,99	78,87	96,16	3,00	62,88	181,35	113,03	37,75	36,80
Run Off	26,26	-63,79	337,21	46,96	151,27	181,00	34,77	92,92	430,87	120,36	-14,50	23,03
Recharge Potential Area	24.816.903											
Infiltration or Recharge Groundwater(liter/month)	16,4	-9,9	81,8	43,1	54,8	66,8	52,8	43,7	126,0	78,5	26,2	25,6
Recharge Groundwater Volume	408.078.827	0	2.030.649.630	1.069.134.916	1.360.144.386	1.658.273.071	1.310.293.698	1.084.397.312	3.127.558.849	1.949.298.715	650.938.822	634.652.464
Total Recharge Groundwater Volume (liter/ year)	15.283.420.689											
Total Recharge Groundwater Volume (m3/ year)	15.283.421											

Figure 8: 1st Method's calculation to estimate Recharge to ground water

DM : Dry Month

WM : Wet Month

PET : Potential Evapotranspiration for 30 days which 12 hr/day sun irradiation

m : Estimate the surface not covered by plants

ΔE : The difference between potential evapotranspiration and limited evapotranspiration (mm/month)

LE : Limited Evapotranspiration

K : Porosity (%)

Cn : Coefficient for n month

Vn : Storage volume n month (mm/month)

2*K : Coefficient groundwater flow (assumed constant every month)

3.3.2 Method 2 (Mean annual groundwater recharge)

The following equation is used to forecast the annual recharge potential of the Lahendong geothermal field:

$$R = A \; x \; P_A \; x \; c$$

R = mean annual groundwater recharge (m^3/year)
A = surface area of recharge zone (km^2)
P_A = mean annual precipitation recharge zone (mm/year)
c = recharge coefficient for the area (%)

The recharge coefficient value normally is determined by conducting an analogy to the research of McDonald (1989) on young volcanic sediments which have similar formations to those of the Lahendong geothermal field. They classify the young volcanic sediments into three zones :

1. Top slope (slope = 50%), recharge coefficient = 25% - 50%
2. Middle slope (slope = 20% - 30%), recharge coefficient = 25%
3. Lower slope and foothills elevation < 800 m (slope = 5% - 10%), recharge coefficient = 20% - 25%.

The research region is located in the middle - lower slope zone, which is composed of of andesite, basalt, and some pyroclastic material featuring fractures. The recharge coefficient used in the computation is 26%, hence the recharge potential of the research area is determined as table below:

FID	Recharge Potential Area [A] (m2)	Rainfall [PA] (mm/year)	Rainfall [PA] (liter/m2/year)	Water Availability on Specific Area [A] x [PA] (liter/year)	Slope [c] (%)	Recharge Groundwater [R] (m3/year)
0	351.877	2.415	2.415	849.783.269	26	220.944
1	2.715.920	2.587	2.588	7.026.085.688	26	1.826.782
2	1.681.708	2.323	2.323	3.906.887.661	26	1.015.791
3	499.465	2.140	2.140	1.068.606.362	26	277.838
4	1.034.253	2.140	2.140	2.212.783.514	26	575.324
5	992.663	2.096	2.096	2.080.456.782	26	540.919
6	732.990	2.096	2.096	1.536.225.666	26	399.419
7	1.448.877	2.022	2.022	2.929.991.262	26	761.798
8	357.304	1.095	1.095	391.247.422	26	101.724
9	195.548	1.095	1.095	214.125.128	26	55.673
10	516.240	1.924	1.924	993.246.379	26	258.244
11	197.116	1.924	1.924	379.251.468	26	98.605
12	400.026	1.924	1.924	769.649.113	26	200.109
13	3.763.333	2.323	2.323	8.742.849.317	26	2.273.141
14	548.836	2.323	2.323	1.275.038.019	26	331.510
15	3.062.415	1.915	1.915	5.862.992.588	26	1.524.378
16	6.318.331	2.219	2.219	14.018.008.184	26	3.644.682
Total Recharge Groundwater Volume (m3/ year)						**14.106.879**

Figure 9: 2nd Method's calculation to estimate Recharge to ground water

The first method calculates the amount of water entering groundwater as 15.283.421 m^3/year, while the second way calculates it as 14.106.879 m^3/year. Both methodologies are then used to determine reservoir recharge using the rock porosity (K=8%) methodology, with potential recharge values of approximately 1.122.673 m^3/year and 1.128.550 m^3/year. In simplified terms, the process flow is as follows:

Model simple

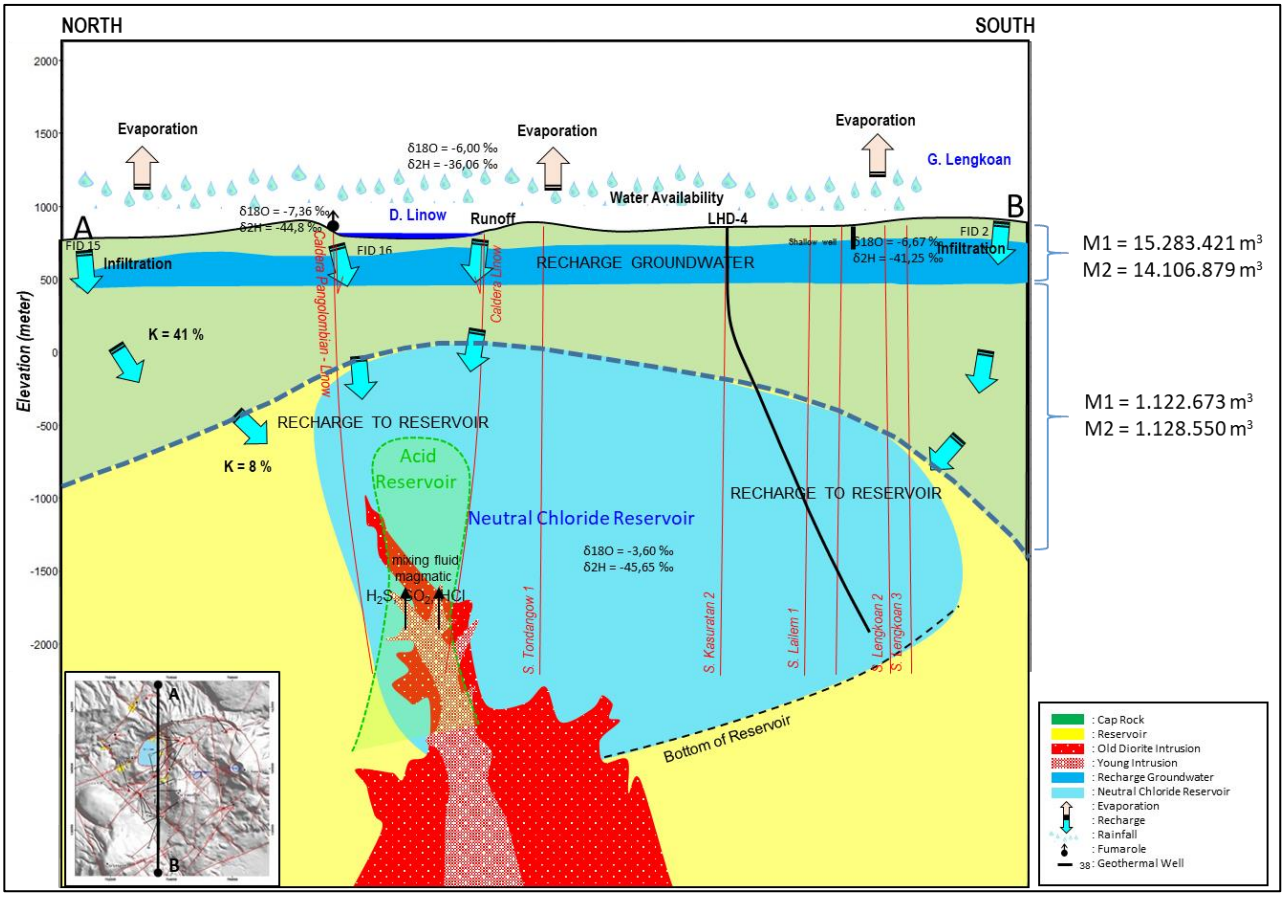

Figure 10: Simplify conceptual recharge flow process to reservoir geothermal in Lahendong

4. CONCLUSION

The conclusions of estimating the potential recharge within one year of monitoring, taking into consideration rain availability, utilizing the fault fracture density approach, and using deuterium and 18-oxygen stable isotopes to derive recharge elevations produce results identical with the simple scenario above 1.125.611 m^3/year of water entering the reservoir corresponds to 1,125 Mton of mass. This is also verified by increases in the average microgravity value during in the Lahendong area where there is an average mass of 1,225 Mton/year added from water recharge.

REFERENCES

Blasch KW, B. J. (2007). Distinguishing sources of ground water recharge by using δ2H and δ18O. *Ground Water 45*, 294 -308.

Clark ID, F. P. (1997). Environmental isotopes in hydrology. *Lewis*.

Craig, H. (1961). Isotopic variation in meteoric waters. *Science 133*, 1702 - 1703.

Darling, W. A. (1961). Stable isotopic aspects of fluid flow in the Krafla, Namafijall and Theistareykir geothermal systems of northeast Iceland. *Chem Geol 76*, 197 - 213.

Desphande RD, B. S. (2003). Distribution of oxygen and hydrogen isotopes in shallow groundwaters from Southern India: influence of a dual monsoon system. *J Hydrol 271*, 226 - 239.

Duplessy J, L. J. (1980). Continental climatic variations between 130,000 and 90,000 years BP. *Nature 226*, 631 - 633.

Gammons CH, P. S. (2006). The hydrogen and oxygen isotopic composition of precipitation, evaporated mine water, and river water in Montana, USA. *J Hydrol 328*, 319 - 330.

Gat, J. (1980). The isotopes of hydrogen and oxygen in precipitation. *Hanbook of environmental isotopes geochemistry*, 21 - 47.

Gat, J. (1996). Oxygen and hydrogen isotopes in the hydrologic cycle. *Annu Rev Earth Planet Sci* , 225 - 262.

Gibson JJ, E. T. (2005). Progress in isotope tracer hydrology in Canada. *Hydrol Process 19*, 303 - 327.

Hennig GJ, G. R. (1983). Speleothems, travertines, and paleoclimates. *Quat Res 20*, 1 - 29.

Koestono H, S. E. (2010). Geothermal model of the Lahendong geothermal field, Indonesia. *World Geothermal Congress.* Bali, Indonesia.

Kumar US, S. S. (2008). Recent studies on surface water–groundwater relationships at hydro-projects in India using environmental isotopes. *Hydrol Process 22*, 4543 - 4553.

Li F, P. G. (2008). Recharge source and hydrogeochemical evolution of shallow groundwater in a complex alluvial fan system, southwest of North China Plain. . *Env Geol 55*, 1109–1122.

Palmer PC, G. M. (2007). Isotopic characterization of three groundwater recharge sources and inferences for selected aquifers in the upper Klamath Basin of Oregon and California, USA. . *J Hydrol* , 336:17–29.

Payne BR, Y. Y. (1974). Environmental isotopes as a hydrogeological tool in Nicaragua Isotope Techniques in Groundwater Hydrology. *IAEA*, (pp. 193–201). Viena.

Perry EC, G. T. (1980). H, O, S isotopic study of the groundwater in the Cambrian–Ordovician aquifer system of northern Illinois. *In: Perry EC, Montgomery CW (eds) Isotope studies of hydrologic processes Northern Illinois University*, (pp. 34 - 43). Illino.

Sakai H, M. O. (1977). Stable isotopic studies of Japanese geothermal system. . *Geothermics 5*, 97–124.

Senturk F, B. S. (1970). Isotope techniques applied to groundwater movement in the Konia plain. In: Isotope hydrology. *IAEA*, (pp. 153–161). Vienna.

Siahaan, E. S. (2005). Tectonism and volcanism study in the Minahasa compartment of the north arm of Sulawesi related to Lahendong geothermal field, Indonesia. *World Geothermal Congress*, (p. 5). Turkey.

Van Der Straaten CM, M. W. (1983). Stable isotopic composition of precipitation and climatic variability. In: Palaeoclimates and Palaeowater. *IAEA*, (pp. 53–64). Vienna.

Vandenschrick G, v. W.-B. (2002). Using stable isotope analysis (δD and δ18O) to characterise the regional hydrology of the Sierra de Gador, south east Spain. . *J Hydrol 265*, 43–55.

Widagda L, J. I. (2005). Recharge Calculation of Lahendong Geothermal Field in North Sulawesi - Indonesia. *World Geothermal Congress.* Antalya, Turkey.

Yurtesever Y, G. J. (1981). Atmospheric waters. In: Gat JR, Gonfiantini R (eds) Stable isotope hydrology: deuterium and oxygen-18 in the water cycle. *IAEA Technical Report Series No. 210*, (pp. 103–142).

Z, S. (2007). Principles of stable isotope geochemistry. *Pearson Prentice Hall*, (p. 344). New Jersey.